

Alexandra Kuzyk

**Title:** Chromosome territory position of chromosome X and 11 is non-random and cell-type specific in mouse cells of B cell lineage.

**By:** Alexandra Kuzyk

**Supervisor:** Dr. Sabine Mai

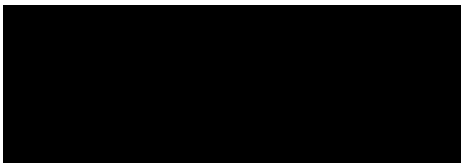
**Department Affiliations:** Biochemistry and Medical Genetics

**Summary:**

The interphase nucleus of a cell is organized into non-random, cell-type specific chromosome territories (CTs). In lymphocytes, a gene-density correlated radial arrangement has been identified, with gene-dense CTs located more in the nuclear interior and gene-poor CTs located towards the periphery. However, other factors such as chromosome size, transcription and interactions of the nuclear membrane and matrix are also involved in the final arrangement of CTs within a nucleus. In this project, the CTs of chromosome 11 and X were studied in five different cell types of mouse B cell lineage: diploid preB cells, primary B cells of [T38HxBALB/c]N wild-type mice, primary B cells of [T38HxBALB/c]N with *recT(X;11)* mice, primary B cells of BALB/c mice and a Wehi 231 mouse B lymphoma line. These two chromosomes have not been studied before in the mouse. 3D FISH experiments that labeled the CTs of chromosome 11 and X with chromosome-specific paints were carried out for each cell type. The karyotype regarding these two chromosomes and specificity of the chromosome paints was first confirmed through 2D FISH experiments. The radial distance from the centre of each CT to the centre of the nucleus was measured using AxioVision 4.8 software. The results show a non-random, statistically significant and cell-type specific nuclear distribution of these two chromosomes. Altered nuclear positions of translocation chromosomes in normal healthy mice and as a result of tumorigenesis were observed in the primary B cells of [T38HxBALB/c]N with *recT(X;11)* mice and in the Wehi 231 mouse B lymphoma line, respectively.

**Acknowledgements:**

Stipendiary support for the student and Dr. Mai's research is supported by a grant from the CIHR.



## Introduction

In the interphase nucleus, chromosomes decondense into chromosome territories (CTs) that occupy distinct volume regions.<sup>1</sup> CT position is established early in G1 and is stable throughout interphase.<sup>2</sup> Large-scale movements of CTs relative to each other are rare until mitosis<sup>3</sup>, with most undergoing limited diffusion during interphase.<sup>4</sup> CTs have preferred neighbors that are cell-type specific.<sup>5</sup> It is now known that decoding chromatin does not explain everything, but rather epigenomes in multi-cellular organisms also depend on higher-order chromatin organization and nuclear architecture.<sup>6</sup> At this time, the ultrastructure of CTs is not fully understood. ~1Mbp chromatin domains are known to be the basic structural unit of CTs.<sup>7</sup> These domains are thought to be built from small-scale chromatin loops of ~1000kbp. Many ~1Mbp are joined to form clumps of chromatin. CTs are composed of the higher-order folding of these chromatin clumps. The compactness of the CT can vary based on its function. For example, the Barr body inactive X chromosome is more compact than the active X chromosome.<sup>8</sup> CTs exist for physical reasons as highly crowded, long polymer molecules maximize entropy by forming intramolecular territories and limiting intermingling.<sup>9</sup> CTs have been visually proven for decades and recently computer modeling support has been generated.<sup>10</sup>

Different models have been proposed to explain CT architecture. The first, the Interchromosomal Domain (ICD) model, was hypothesized by Zirbel in 1993.<sup>11</sup> He stated the ICD was a space mainly around CTs with little penetrance into their interior. Genes were said to be transcribed in the decondensed region of chromatin at the CT periphery and RNA transcripts were released into the ICD. However this model fell out of favor as genes were found to be transcribed both inside and on the outside of a CT.<sup>12,13</sup> This finding led to the proposal of the CT Interchromatin Compartment model.<sup>7,14</sup> This model stated that CTs are spatially associated with a second contiguous 3D spatial network, the interchromatin compartment (IC). The IC begins at nuclear pores and expands as channels between higher-order chromatin. The IC is DNA free and harbors splicing speckles and nuclear bodies. A thin layer of decondensed chromatin, the perichromatin region, separates the IC from condensed chromatin. The perichromatin region is the major area for transcription, splicing, DNA replication and repair.<sup>15</sup> Although the CTIC model is the most widely accepted a couple others are also proposed. The Interchromatin Network model<sup>16</sup> states that chromatin fibers and loops intermingle in a uniform way in the interior of individual CT and between neighboring CT. This intermingling makes the distinction of interior and periphery of CTs meaningless. The Giant-loop model<sup>17,18</sup> states that giant loops of chromatin can reach from on CT and expand across nuclear space to carry genes to remote sites for co-regulation or repression. However, this model argues for no DNA free space, which has been proven to be present by electron microscopy.<sup>14,19</sup>

CTs are studied through microscopic and non-microscopic methods. Microscopy is needed to see chromatin structure. This is mainly done through fluorescence *in situ* hybridization (FISH) techniques that can measure mean spatial distance between two loci. Traditional problems with FISH have been resolution limitations; however, this is being solved with the invention of new ultra-high resolution microscopes.<sup>20,21</sup> Non-microscopic methods are needed to determine the exact interacting sequences of CTs. The main method for this type of study is chromosome conformation capture (3C) that can determine the probability of contact between two loci that are a 'x' distance apart.<sup>10</sup> The limitation of 3C is that the area of interest has to be

known; recently the invention of Hi-C<sup>22</sup> avoids this issue because it can identify long-range interactions for the whole genome. Because Hi-C relies on the successful ligation of only spatially adjacent chromatin segments, over-interpretation of interacting sequences can occur if ligation between non-adjacent segments; therefore comparison of Hi-C results with other data is important to avoid this problem.

The arrangement of CTs is a topic of great debate. There have been many theories proposed about why CTs are found in a non-random region of an interphase nucleus and why CTs have non-random neighbors; however, it is important to remember that although there are many theories about how the CTs are arranged and interact, most groups agree that more than one factor contributes to the final arrangement. There has been much study into how CT gene-density and size affects its interphase position. It has been shown multiple times that a non-random gene-density correlated radial arrangement is found in human lymphocytes<sup>23,24</sup> and that a non-random chromosome size correlated radial arrangement is found in ellipsoid fibroblasts.<sup>25</sup> However, in fibroblasts a gene-density pattern was found at the sub-chromosome level with Alu (gene dense) sequence-rich chromatin in the nuclear interior.<sup>25</sup> Human lymphocyte chromosomes 18 and 19 are of similar size but dissimilar gene content; chromosome 18 is gene-poor and found at the nuclear periphery whereas chromosome 19 is gene-rich and found in the nuclear interior.<sup>26</sup> Bladder cells were discovered to have a weak linear relationship for gene-density and size correlated radial arrangements but the ratio of density:size showed a very strong correlation<sup>27</sup>; this study demonstrates that both gene-density and size of CTs many have a significant role in CT arrangement. Evolutionary studies have also demonstrated the importance and conservation of a radial CT arrangement.<sup>28</sup> Lymphoblastoid cells from human, orangutan and gibbon showed an evolutionary conserved gene-density related arrangement of homologous sequences. Although there was no conserved size-related radial pattern in fibroblasts, when cells with similar-sized chromosomes were examined (from Wolf's guenon), a gene-density radial relationship was observed; therefore it was proposed that geometrical constraints account for differences in radial distribution.

Transcription is also thought to be an important factor in CT arrangement. Transcriptionally active alleles are usually found on the edge of a CT or outside of it altogether, whereas inactive alleles are found embedded inside the CT.<sup>29</sup> Gene-rich loops containing sections of the major histocompatibility complex on human chromosome six have been found to extend out of their CT at a greater frequency when their transcription is increased.<sup>30</sup> In the past, the nuclear periphery has been thought to be an area of transcriptional repression as this is where constitutive heterochromatin is usually found. In contrast, early replicating transcriptionally active euchromatin is usually found in the nuclear interior. However, experiments which identified nascent RNA production, found transcription to occur through the nucleus.<sup>31</sup> In mice, the interferon  $\gamma$  locus is found at the nuclear periphery whether or not it is transcriptionally active. Artificially tethering chromatin regions in mammalian cells to the membrane only down-regulated specific genes (*cxc11* and *cxc15*).<sup>32,33</sup> Also, nuclear pore complexes are emerging as a region of increased transcription.<sup>34</sup> Certain genes are repositioned to the nuclear interior from the periphery during transcriptional activation.<sup>35,36,37</sup> Others move to the interior with increased expression and to the periphery with repression.<sup>38,39,50</sup> One study tried to reposition the *Mash1* locus to the interior from the periphery but this did not initiate transcription.<sup>41</sup> Another study attempted to upregulate gene expression by looping out a gene from its CT but it was not

successful.<sup>29</sup> It is hypothesized that the nuclear interior may be more important in acquiring a high transcriptional rate rather than initiating the event itself.<sup>42</sup> Transcription occurs in transcription factories that are attached to the nucleoskeleton throughout the nucleus.<sup>42</sup> It has been found that the genes *Myc* and *Igh* co-transcribe in a single transcription factory in mouse lymphocytes; this is important as these two genes are often involved in translocation events in lymphoma.<sup>43</sup> It is possible that functionally related genes may meet to be co-transcribed; therefore, gene position in the nucleus (and in turn CT position) may be influenced by transcription factory location. Most likely whether genes are positioned near their transcription factory or whether they need to migrate out of the CT to reach their transcription factory is dependent on cell-type and locus-specific factors. The nuclear matrix also plays an important role in organizing and binding chromatin through binding proteins such as lamins and telomeres.<sup>44</sup> It has been hypothesized that disruption of the matrix can alter both chromosome and chromatin organization.<sup>42</sup>

Many groups believe the non-randomness of a DNA interaction between two fragments is not only due to the genomic proximity between them but must also be due to specific DNA binding factors. Hi-C combined with ChIP experiments have been used to identify these factors.<sup>45</sup> CCCTC-binding factor is a highly conserved protein and has a significant role in organizing long DNA loops within chromosomes at specific loci. Repeat sequences such as telomeres and centromeres also interact to form 'hubs' made from different CT.<sup>45</sup> The arrangement of CT may also be a result of cellular preservation or function. It was found that chromosomes are non-randomly always closer to a heterologue than a homologue.<sup>27</sup> The conservation of homologue proximity may be evolutionally important to avoid homologous recombination (and loss of heterozygosity) and damaging both copies of a chromosome from a single stress. One interesting study demonstrated that CTs reorganize during terminal differentiation in rod cells of retinal tissue.<sup>46</sup> Nocturnal animals showed an inversed heterochromatin and euchromatin arrangement with heterochromatin in the interior of the nucleus and euchromatin at the periphery. This was thought have come to be as an adaptation to lower light conditions as the increased refractive index of condensed heterochromatin makes night vision clearer when heterochromatin is in the nuclear interior.

In my project I examined the chromosome territory position of chromosome X and 11 in mouse B lineage cells. To date, no previous studies have looked at these two chromosomes in the mouse. The goal of my project was to understand the position of these two chromosomes in cell lines and primary mouse cells of B cell lineage. Using FISH techniques and computer analysis, chromosome positions in diploid preB cells, primary B cells of [T38HxBALB/c]N wild-type mice, primary B cells of [T38HxBALB/c]N with repT(X;11) mice, primary B cells of BALB/c mice and a Wehi 231 mouse B lymphoma line were examined. I demonstrate that chromosome territory position is non-random and cell-type specific in different species of lymphocytes.

## Materials and Methods

The techniques of 2D and 3D fluorescent *in situ* hybridization were used to visualize chromosomes in metaphases and the interphase nucleus, respectively. Chromosome paints for chromosome 11 and chromosome X were purchased from Applied Spectral Imaging (Vista, CA).

Nuclei were visualized following counterstaining with 4',6'-diamidino-2-phenylindole (DAPI). Three independent experiments were carried out for the following cell combinations; i) diploid preB cells; ii) primary B cells of [T38HxBALB/c]N wild-type mice<sup>47</sup>; iii) primary B cells of [T38HxBALB/c]N with repT(X;11) mice (Wiener 2010); iv) primary B cells of BALB/c mice; v) a Wehi 231 mouse B lymphoma line.<sup>48</sup>

Metaphases were prepared for each of the cell types according to Mai and Wiener.<sup>49</sup> Briefly, the chromosomes underwent drop fixation using a 3:1 methanol:acetic acid solution. Then 30 $\mu$ L of the chromosome-fixative solution was dropped onto a cooled slide, heated to 38°C, dipped into acetic acid and heated again until the slide was dry. To visualize the spreads, the slides were stained with Giemsa (Gibco). At least 20 metaphases with non-overlapping chromosomes were examined in three independent experiments. Our previous studies have indicated that this number suffices for statistical significance.<sup>50</sup> Briefly, the slides were treated with RNAase A, followed by a pepsin/HCl treatment; next the slides were fixed in formaldehyde, denatured at 70°C in formamide and finally, incubated overnight in a 37°C humidified atmosphere with the denatured chromosome paints. 2D imaging and acquisition were performed using DAPI filter (for nuclear DNA staining), Cy3 filter (for detection of chromosome 11 signals), FITC filter (for detection of chromosome X signals) and Zeiss AxioVision 4.8 software (Carl Zeiss Canada, Toronto, ON).

Cells were 3D-fixed according to our published protocols.<sup>51,52,53</sup> Briefly, the slides were fixed in formaldehyde and then incubated in glycerol for an hour, followed by a freeze-thaw treatment with liquid nitrogen. After a HCl incubation, the slides were equilibrated for an hour in formamide, followed by a denaturation in formamide at 70°C. Finally the slides were incubated overnight in a 37°C humidified atmosphere with the denatured chromosome paints. 3D imaging and acquisition were performed as similarly to the 2D procedure. 80 z-stacks at 200nm each, with x,y: 107nm, z: 200nm were acquired. The images were deconvolved using the constrained iterative algorithm.<sup>54</sup> Thirty nuclei per cell type and experiment were analyzed. Our previous studies have indicated that this number suffices for statistical significance.<sup>51</sup> Qualitative analysis of 3D chromosome positions was done first, followed by quantitative analysis. The distance of each chromosome from the centre of the nucleus was measured using the "Circle Out-In" measure function in the AxioVision 4.8 software.

---

## Results

Metaphase spreads for each cell type were prepared, in three independent experiments, and subsequently underwent a FISH protocol with chromosome paints which labeled all chromosome 11 and X regions (see Materials and Methods). The results can be seen in Figure I with chromosome 11 labeled in red and chromosome X in green. 103 metaphases from three diploid preB cell passages (passage #5, 18 and 42) were imaged (greater than 20 images per sample); as expected, every metaphase had 40 chromosomes, two each of chromosome 11 and X (Figure Ii). 64 metaphases from primary B cells of three [T38HxBALB/c]N wild-type mice were imaged; also as expected each spread had 40 chromosomes, two each of chromosome 11 and X (Figure Iii). 65 metaphases from primary B cells of three [T38HxBALB/c]N with repT(X;11) mice were imaged; every spread had the expected karyotype of 40 chromosomes with one 11, X, large T(11;X) and small T(X;11) chromosome (Figure Iiii). 20 metaphases from primary B cells

of one BALB/c mouse were imaged; each spread accurately had 40 chromosomes, two each of chromosome 11 and X (Figure Iiv). 25 metaphases from a Wehi 231 mouse B lymphoma line were imaged; this cell line has an unstable karyotype with metaphases ranging from 37 to 41 chromosomes. Each metaphase had two normal chromosome 11s, one small chromosome 11 (probable product of a deletion) and one or two X chromosomes (Figure Iv).

Interphase nuclei for each cell type were prepared, in three independent experiments, for 3D FISH experiments which labeled in CT position of chromosomes 11 and X (see Materials and Methods). The results can be seen in Figure II with chromosome 11 labeled in red and chromosome X in green. The position of each CT was categorized as in the centre of the nucleus, at the periphery or in between these two positions (middle); these positions are illustrated in Figure Iii. The distance from the centre of the nucleus for each CT was then measured with a function of the AxioVision program which outlined the circular nucleus, identified its centre and calculated the straight line distance from the centre to the middle of a CT. These values were assigned to a category as follows: <33.4% as centre, 33.4-66.6% as middle and >66.6% as periphery of the nucleus. Tables and graphs of these measurements are shown in Figures III, IV and V.

91 cells from three diploid preB cell passages (passage #24, 43 and 50) were imaged (30 or more per slide). As predicted from the 2D metaphase FISH results, two similar sized regions of each chromosome 11 and X were identified (Figure Iiii). A trend was seen with regards to the position of both chromosomes. Most were found at the periphery of the nucleus: 57.1% of chromosome 11 and 75.8% of chromosome X. Very few chromosome 11 and X CTs were found in the centre of the nucleus: only 2.2% of chromosome 11 and X. Chromosome 11 CTs showed a peak in their radial distribution at 70% of the cell's radius whereas the peak for chromosome X data was more prominent at 80% (Figure IIIi).

91 cells from three [T38HxBALB/c]N wild-type mice were imaged. Similar to the 2D metaphase FISH results, two similar sized regions of each chromosome 11 and X were identified (Figure Iiii). The majority of chromosome 11 CTs, 61.0%, were found in the middle category of radial distribution. In contrast, the majority of chromosome X CTs, 68.1%, were found at the periphery of the nucleus. Very few chromosome 11 and X CTs were found in the centre of the nucleus: only 3.8% of chromosome 11 and 1.1% of X. The chromosome X CT showed a peak in its radial distribution around 80%. However, the CTs of chromosome 11 had a broad peak from 50-70% (Figure IIIii).

100 cells from three [T38HxBALB/c]N with rcpT(X;11) mice were imaged. The small T(X;11) CT was visible in only 11/100 cells (Figure Iiv), which therefore had three regions labeled with chromosome 11 paint (corresponding to one each of chromosome 11, T(X;11) and T(11;X). In all the other cells, two regions labeled with chromosome 11 paint were identified, the region attached to a chromosome X labeled region corresponds to the T(11;X) chromosome (Figure Iiv). The second region labeled with chromosome X paint corresponds to the chromosome X CT. Chromosome 11 was found in 41.0% of cells at the periphery, 50.0% in the middle region and 9.0% in the centre. CT X was found in 61.0% of cells at the periphery, 30.8% in the middle region and 1.1% in the centre. The long T(11;X) CT was found in 51.0% of cells at the periphery, 43.0% in the middle region and 6.0% in the centre. The small T(X;11) CT was

found in 81.8% of cells in centre and 18.2% in the middle region. As seen in Figure IIIiii, the most frequent radial distance was approximately 80% for all CT but T(X;11) which was found most frequently at about 30%.

30 primary B cells from one BALB/c mouse were imaged. As expected from the 2D metaphase FISH results, two similar sized regions of each chromosome 11 and X were seen (Figure IIvi). The majority of both chromosome 11 and X were found at the periphery, 56.7 and 58.3% respectively, with 40.0 and 35.0% found in the middle region and 3.3 and 6.7% occurring in the centre of the nucleus. Figure IIIiv summarizes the CT distribution in these cells.

31 cells from a Wehi 231 mouse B lymphoma line were imaged. Results were similar to those seen from the 2D FISH experiments. Two similar sized chromosome 11 CT, one small (deletion) chromosome 11 CT and one or two chromosome X CTs were identified in the nuclei (Figure IIvii). The deletion chromosome 11 CT was found in 77.4% of cells in the middle region, 16.1% in the centre and only 6.5% at the periphery. The majority of the normal chromosome 11 and chromosome X CTs were found at the periphery (77.4 and 85% respectively), with 22.6 and 15.0% in the middle region and none found in the centre. The radial distance of the CT was 90% of the cell's radius for about 40% of chromosome X CTs and 20% of normal chromosome 11 CTs (Figure IIIv). The radial distance of the deletion 11 CT peaked around 42% of the cell's radius.

Statistical analysis was performed on the data for the nuclear radial positioning of the CTs. A GLM Procedure which compared the chromosome 11 CT for all 5 cell types found a significant difference between all cell types for this CT ( $p < 0.0001$ ). The same test was also done to compare the chromosome X CT in all 5 cell types and a significant difference ( $p < 0.0001$ ) was found.

A Least Squares Means test was done to compare every cell-cell combination for significant differences in their nuclear positioning of the chromosome 11 CT. The comparison of primary B cells of BALB/c mice with all other cell types yielded the following results: a significant difference between primary B cells of [T38HxBALB/c]N with rcpT(X;11) mice ( $p = 0.0027$ ), primary B cells of [T38HxBALB/c]N wild-type mice ( $p = 0.0016$ ) and Wehi 231 mouse B lymphoma line cells ( $p = 0.0004$ ) but no significant difference with diploid preB cells ( $p = 0.7490$ ). A similar comparison of diploid preB cells with all other cell types yielded the following new information: a significant difference between primary B cells of [T38HxBALB/c]N with rcpT(X;11) mice ( $p = 0.0004$ ), primary B cells of [T38HxBALB/c]N wild-type mice ( $p < 0.0001$ ) and Wehi 231 mouse B lymphoma line cells ( $p < 0.0001$ ). The comparison of primary B cells of [T38HxBALB/c]N with rcpT(X;11) mice with all other cell types yielded the following new results: a significant difference with Wehi 231 mouse B lymphoma line cells ( $p < 0.0001$ ) but no significant difference with primary B cells of [T38HxBALB/c]N wild-type mice and ( $p = 0.8685$ ). The comparison of primary B cells of [T38HxBALB/c]N wild-type mice with all other cell types yielded the following new finding: a significant difference between Wehi 231 mouse B lymphoma line cells ( $p < 0.0001$ ).

The results for the Least Squares Means test which compared every cell-cell combination for significant differences in their nuclear positioning of the chromosome X CT are as follows.

The comparison of primary B cells of BALB/c mice with all other cell types yielded the following results: a significant difference between diploid preB cells ( $p = 0.0074$ ) and Wehi 231 mouse B lymphoma line cells ( $p < 0.0001$ ) but no significant difference with [T38HxBALB/c]N with *recT(X;11)* mice ( $p = 0.9241$ ) or [T38HxBALB/c]N wild-type mice ( $p = 0.1830$ ). A similar comparison of diploid preB cells with all other cell types yielded the following new information: a significant difference with primary B cells of [T38HxBALB/c]N with *recT(X;11)* mice ( $p = 0.0021$ ) and Wehi 231 mouse B lymphoma line cells ( $p = 0.0078$ ) but no significant difference with [T38HxBALB/c]N wild-type mice ( $p = 0.0546$ ). The comparison of primary B cells of [T38HxBALB/c]N with *recT(X;11)* mice with all other cell types yielded the following new results: a significant difference between Wehi 231 mouse B lymphoma line cells ( $p < 0.0001$ ) but no significant difference with primary B cells of [T38HxBALB/c]N wild-type mice and ( $p = 0.1423$ ). The comparison of primary B cells of [T38HxBALB/c]N wild-type mice with all other cell types yielded the following new finding: a significant difference with Wehi 231 mouse B lymphoma line cells ( $p = 0.0001$ ).

A T-Test Procedure found a significant difference between the radial positions of the two translocation chromosomes in the primary B cells of [T38HxBALB/c]N with *recT(X;11)* mice ( $p$ -value  $< 0.0001$ ). Another T-Test Procedure found a significant difference between the normal and deletion chromosome 11s in the Wehi 231 mouse B lymphoma line cells ( $p$ -value  $< 0.0001$ ).

## Discussion

Although chromosome 11 and X have not been studied in mice before, their CTs were expected to be non-random and cell-type specific like all other CTs. In this project, the radial distribution of these two CTs was studied in five cell types of mouse B cell lineage: diploid preB cells, primary B cells of [T38HxBALB/c]N wild-type mice, primary B cells of [T38HxBALB/c]N with *recT(X;11)* mice, primary B cells of BALB/c mice and a Wehi 231 mouse B lymphoma line. Chromosome 11 and X were chosen because X acts as a control to chromosome 11 which contains the genes involved in creating a small translocation chromosome that helped identify the tumor accelerating chromosomal regions necessary for tumorigenesis in fast-onset plasmacytomas in mice.<sup>47</sup>

Lymphocytes are spherical cells previously found to have a gene-density related radial arrangement of the CTs.<sup>23,24,26</sup> Chromosome 11 has a total estimated size of 122Mbp; chromosome X is slightly larger with 161.5Mbp.<sup>55</sup> The gene density of chromosome X is 6.54 (units of exons/CDS), a density less than that of chromosome 11 which is 8.57.<sup>55</sup> This makes chromosome 11 the second most gene-dense chromosome and chromosome X third from least gene-dense chromosome in the mouse genome.

Two copies of chromosome X were found in all cell types except for about half of the Wehi 231 mouse B lymphoma line cells that lost one copy; however, it is common for tumors to lose sex chromosomes.<sup>56,57</sup> The same trend in radial distribution of chromosome X was identified in all cell types with the great majority at the nuclear periphery, less in the middle position and very few copies found in the centre of the cell (Figure IVi). There was a statistically significant difference in the nuclear position of chromosome X between all five cell types ( $p < 0.0001$ ). These consistent results justify the decision to use chromosome X as a control. Also these

findings support theories that state large and gene-poor chromosomes are found at the nuclear periphery. The CT of chromosome 11 was found to have a less peripheral radial distribution than the CT of chromosome X, in all cell types. As a smaller, more gene-dense chromosome, these results agree with previous work.<sup>1,26</sup> Although the majority of chromosome 11 CTs were still found in a peripheral position in diploid preB cells, primary B cells of BALB/c mice and a Wehi 231 mouse B lymphoma line cells, the majority were found in a middle position in both primary B cells of [T38HxBALB/c]N wild-type and *recT(X;11)* mice (Figure IVB). There was a statistically significant difference in the nuclear position of chromosome 11 between all five cell types ( $p < 0.0001$ ).

However, when only cell-cell combinations were compared a significant difference in chromosome X was only seen in between some of these cells (see Results). CT X position was significantly different between diploid preB cells and all other cell types; the same is true for Wehi 231 mouse B lymphoma line cells. Primary cells from the two T38H mouse types were not significantly different with each other or with primary B cells of BALB/c mice. Therefore the chromosome X CT position was only significantly different between cell lines and primary cells. Statistical analysis of CT 11 revealed only two cell-cell combinations that were not significantly different: between primary B cells of BALB/c mice and diploid preB lymphocytes and between primary B cells of [T38HxBALB/c]N wild-type and *recT(X;11)* mice.

Primary B cells of [T38HxBALB/c]N wild-type and *recT(X;11)* mice show a very similar distribution of their chromosome 11 and X CTs even though two translocation chromosomes are also present in the *recT(X;11)* mice. In the category order of periphery, middle and centre radial distribution, the values for CTs are as follows: for chromosome 11 in the wild-type mouse - 35.2, 61.0 and 3.8%; for chromosome 11 in the translocation mouse - 41.0, 50.0 and 9.0%; for chromosome X in the wild-type mouse - 68.1, 30.8 and 1.1%; for chromosome X in the translocation mouse - 61.0, 37.0 and 2.0%. The long T(11;X) translocation chromosome is also found more often at the periphery than any other radial position: 51.0% versus 43.0% in the middle and 6.0% in the centre categories. However, the small T(X;11) translocation chromosome is found in 81.8% of cells in the nuclear interior, with 18.2% in the middle position and none found at the periphery. An explanation for this finding could be that the genes found on this chromosome require a higher rate of transcription. Therefore it could have moved from the more peripheral position of the other translocation chromosome (T(11;X) and the normal 11 and X CTs, towards the nuclear interior - an area of greater transcription activity.<sup>36,37,38</sup> It is known that the genes on the small translocation chromosome are important in the tumorigenesis of mouse plasmacytoma<sup>47</sup>, which supports possible increased transcriptional activity. An interesting finding in the interphase nuclei of the *recT(X;11)* mice cells is that in most cells, the CT of the small translocation chromosome is not visible; it is possible that both translocation chromosomes are co-localized in these cells for not yet understood reasons. Work by the Ried group has illustrated such findings as artificially introducing a third chromosome and following its localization in the nucleus, revealed that it paired with one of the existing chromosomes.<sup>58</sup>

The Wehi 231 mouse B lymphoma line demonstrates how CT positions can be altered during tumorigenesis. Two normal copies of chromosome 11 were identified along with a smaller chromosome 11 that probably underwent a deletion. Figure V shows how this alteration greatly changed the distribution of the chromosome 11 CT; a significant difference ( $p < 0.0001$ )

was found between the normal and deletion chromosome 11. The normal chromosome 11 was found in 77.4% of cells at the periphery and in 22.6% in a middle position. The deletion chromosome 11 was found in 77.4% of cells in the middle position and in only 6.5% of cells at the periphery. Although it is not known why this change occurred, it can be hypothesized the more interior location is a result of the chromosome's smaller size, an increased rate of transcription necessary for this chromosome and/or the deletion may have caused an increase in the chromosome's gene density.

In each cell type studied in this project, a unique non-random radial distribution was observed for chromosome 11 and X CTs. The consistently more peripheral position of chromosome X coincides with it being a larger, less gene-dense CT than chromosome 11. The significance of chromosome aberrations in altering the CT position was observed for both translocation and deletion chromosomes. Also it was shown that each type of cell of B lineage had a statistically significant, different, cell-type specific radial distribution of these two CTs. Although the exact mechanisms are not known, different reasons for the non-random distribution of the chromosome 11 and X CTs in each of these cell types was proposed.

## References

1. Cremer, T.; Cremer, M.; Dietzel, S. et al. Chromosome territories – a functional nuclear landscape. *Curr Opin Cell Biol.* (2006). 18(30): 307-16.
2. Thomson, I.; Gilchrist, S.; Bickmore, W.A. et al. The radial positioning of chromatin is not inherited through mitosis but is established de novo in early G1. *Curr Biol.* (2004). 14(2): 166-72.
3. Lucas, J.N.; Cervantes, E. Significant large-scale chromosome territory movement occurs as a result of mitosis, but not during interphase. *Int J Radiat Biol.* (2002). 78(6): 449-55.
4. Marshall, W.F.; Straight, A.; Marko, J.F. et al. Interphase chromosomes undergo constrained diffusional motion in living cells. *Curr Biol.* (1997). 7(12): 930-9.
5. Marella, N.V.; Bhattacharya, S.; Mukherjee, L. et al. Cell type specific chromosome territory organization in the interphase nucleus of normal and cancer cells. *J Cell Physiol.* (2009). 221(1): 130-8.
6. Cremer, T.; Cremer, M. Chromosome territories. *Cold Spring Harb Perspect Biol.* (2010). 2(3): a003889.
7. Albiez, H.; Cremer, M.; Tiberi C. et al. Chromatin domains and the interchromatin compartment form structurally defined and functionally interacting nuclear networks. *Chromosome Res.* (2006). 14(7): 707-33.
8. Lyon, M.F. Sex chromatin and gene action in the mammalian X-chromosome. *Am J Hum Genet.* (1962). 14: 135-48.
9. Marenduzzo, D.; Micheletti, C.; Cook, P.R. Entropy-driven genome organization. *Biophys J.* (2006). 90(10): 2712-21.
10. Mirny, L.A. The fractal globule as a model of chromatin architecture in the cell. *Chromosome Res.* (2011). 19(1): 37-51.
11. Zirbel, R.M.; Mathieu, U.R.; Kurz, A et al. Evidence for a nuclear compartment of transcription and splicing located at chromosome domain boundaries. *Chromosome Res.* 1993. 1(2): 93-106.
12. Cmarko, D.; Verschure, P.J.; Martin, T.E. et al. Ultrastructural analysis of transcription and splicing in the cell nucleus after bromo-UTP microinjection. *Mol Biol Cell.* 1999. 10(1): 211-23.
13. Mahy, N.L.; Perry, P.E.; Bickmore, W.A. Gene density and transcription influence the localization chromatin outside of chromosome territories detectable by FISH. *J Cell Biol.*

2002. 159(5): 753-63.
14. Visser, A.E.; Jaunin, F.; Aten, J.A. High resolution analysis of interphase chromosome domains. *J Cell Sci.* 2000. 113(Pt 14): 2585-93.
  15. Fakan, S.; van Driel, R. The perichromatin region: a functional compartment in the nuclear that determines large-scale chromatin folding. *Semin Cell Dev Biol.* (2007). 18(5): 676-81.
  16. Branco, M.R.; Pombo, A. Intermingling of chromosome territories in interphase suggests role in translocations and transcription-dependent associations. *PLoS Biol.* (2006). 4(5): e138.
  17. Chubb, J.R.; Bickmore, W.A. Considering nuclear compartmentalization in the light of nuclear dynamics. *Cell.* (2003). 112(4): 403-6.
  18. Fraser, P.; Bickmore, W. Nuclear organization of the genome and the potential for gene regulation. *Nature.* (2007). 447(7143): 413-7.
  19. Rouquette, J.; Genoud, C., Vazquez-Nin, G.H. et al. Revealing the high-resolution three-dimensional network of chromatin and interchromatin space. *Chromosome Res.* (2009). 17(6): 801-10.
  20. Schermelleh, L.; Carlton, P.M.; Haase, S. Subdiffraction multicolor imaging of the nuclear periphery with 3D structured illumination microscopy. *Science.* (2008). 320\*5881): 1332-6.
  21. Gustafsson, M.G. Surpassing the lateral resolution limit by a factor of two using structured illumination microscopy. *J Microsc.* (2000). 198(Pt 2): 82-7.
  22. van Berkum, N.L.; Lieberman-Aiden, E.; Williams, L. et al. Hi-C: A method to study the three-dimensional architecture of genomes. *JoVE.* (2010). 39. <http://www.jove.com/index/Details.stp?ID=1869>.
  23. Croft, J.A.; Bridger, J.M.; Boyle, S. et al. Differences in the localization and morphology of chromosomes in the human nucleus. *J Cell Biol.* (1999). 145(6): 1119-31.
  24. Cremer, M.; von Hase, J.; Volm, T. et al. Non-random radial higher-order chromatin arrangement in nuclei of diploid human cells. *Chromosome Res.* (2001). 9(7): 541-67.
  25. Bolzer, A.; Kreth, G.; Solovei, I. et al. Three-dimensional maps of all chromosomes in human male fibroblast nuclei and prometaphase rosettes. *PLoS Biol.* (2005). 3(5): e157.
  26. Tanabe, H.; Habermann, F.A.; Solovei, I. Non-random radial arrangements of interphase chromosome territories: evolutionary considerations and functional implications. *Mutat Res.* (2002). 504(1-2): 37-45.
  27. Heride, C.; Ricoul, M.; Kieu, K. et al. Distance between homologous chromosomes results from chromosome positioning constraints. *J Cell Sci.* (2010). 123(Pt 23): 4063-75.
  28. Neusser, M.; Schubel, V.; Koch, A. et al. Evolutionarily conserved, cell type and species-specific higher order chromatin arrangements in interphase nuclei of primates. *Chromosoma.* (2007). 116(3): 307-20.
  29. Morey, C.; Kress, C.; Bickmore W.A. Lack of bystander activation shows that localization exterior to chromosome territories is not sufficient to up-regulate gene expression. *Genome Res.* (2009). 19(7): 1184-94.
  30. Volpi, E.V.; Chevret, E.; Jones, T. et al. Large-scale chromatin organization of the major histocompatibility complex and other regions of human chromosome 6 and its response to interferon in interphase nuclei. *J Cell Sci.* (2000). 113(Pt 9): 1565-76.
  31. Wansink, D.G.; Schul, W.; van der Kraan, I. et al. Fluorescent labeling of nascent RNA reveals transcription by RNA polymerase II in domain scattered throughout the nucleus. *J Cell Biol.* (1993). 122(2): 283-93.
  32. Finlan, L.E.; Sproul, D.; Thomson, I. et al. Recruitment to the nuclear periphery can alter expression of genes in human cells. *PLoS Genet.* (2008). 4(3): e1000039.
  33. Kumaran, R.I.; Spector, D.L. A genetic locus targeted to the nuclear periphery in living cells maintains its transcription competence. *J Cell Biol.* (2008). 180(1): 51-65.
  34. Akhtar, A.; Gasser, S.M. The nuclear envelope and transcriptional control. *Nat Rev Genet.* (2007). 8(7): 507-17.
  35. Chuang, C.H.; Carpenter, A.E.; Fuchsova, B. et al. Long-range directional movement of an interphase chromosome site. *Curr Biol.* (2006). 16: 825-31.

36. Dundr, M.; Ospina, J.K.; Sung, M.H. et al. Actin-dependent intranuclear repositioning of an active gene locus in vivo. *J Cell Biol.* (2007). 179(6): 1095-103.
37. Lanctot, C.; Cheutin, T.; Cremer, M. et al. Dynamic genome architecture in the nuclear space: regulation of gene expression in three dimensions. *Nat Rev Genet.* (2007). 8(2): 104-15.
38. Brown, K.E.; Amoils, S.; Horn, J.M. et al. Expression of  $\alpha$ - and  $\beta$ -globin genes occurs within different nuclear domains in haemopoietic cells. *Nat Cell Biol.* (2001). 3: 602-6.
39. Kimura, H.; Sugaya, K.; Cook, P.R. The transcription cycle of RNA polymerase II in living cells. *J Cell Biol.* (2002). 159(5): 777-82.
40. Zink, D.; Amaral, M.D.; Engimann, A. et al. Transcription-dependent spatial arrangements of CFTR and adjacent genes in human cell nuclei. *J Cell Biol.* (2004). 166(6): 815-25.
41. Williams, R.R.; Azuara, V.; Perry, P. et al. Neural induction promotes large-scale chromatin reorganization of the Mash1 locus. *J Cell Sci.* (2006). 119(Pt 1): 132-40.
42. Elcock, L.S.; Bridger, J.M. Exploring the relationship between interphase gene positioning, transcriptional regulation and the nuclear matrix. *Biochem Soc Trans.* (2010). 38(Pt 1): 263-7.
43. Osborne, C.S.; Chakalova, L.; Mitchell, J.A. et al. Myc dynamically and preferentially relocates to a transcription factory occupied by Igh. *PLoS Biol.* (2007). 5(8): e192.
44. Elcock, L.S.; Bridger, J.M. Exploring the effects of a dysfunctional nuclear matrix. *Biochem Soc Trans.* (2008). 36(Pt 6): 1378-83.
45. Botta, M.; Haider, S.; Leung, I.X. et al. Intra- and inter-chromosomal interactions correlate with CTCF binding genome wide. *Mol Syst Biol.* (2010). 6: 426-32.
46. Solovei, I.; Kreysing, M.; Lanctot, C. et al. Nuclear architecture of rod photoreceptor cells adapts to vision in mammalian evolution. *Cell.* (2009). 137(2): 356-68.
47. Wiener, F.; Schmalter, A.K.; Mowet, M.R. et al. Duplication of subcytoband 11E2 of chromosome 11 is regularly associated with accelerated tumor development in v-abl/myc-induced mouse plasmacytomas. *Genes Cancer.* (2010). 1(8): 847-58.
48. Mai, S.; Hanley-Hyde, J.; Rainey, G. et al. Chromosomal and extrachromosomal instability of the cyclin D2 gene is induced by myc overexpression. *Neoplasia.* 1999. 1(3): 241-52.
49. Mai, S.; Wiener, F. Murine FISH. In: Beatty B, Mai S, Squire J, editors. A practical approach. Oxford: Oxford University Press; 2002. P.55-76.
50. Guffei, A.; Sarkar, R.; Klewes, L. et al. Dynamic chromosomal rearrangements in Hodgkin's lymphoma are due to ongoing three-dimensional nuclear remodeling and breakage-bridge-fusion cycles. *Haematologica.* (2010). 95(12): 2038-46.
51. Louis, S.; Vermolen, B.; Garini, Y. et al. c-Myc induces chromosomal rearrangements through telomere and chromosome remodeling in the interphase nucleus. *PNAS.* 2005. 102(27): 9613-18.
52. Chuang, T.; Moshir, S.; Garini, Y. et al. The three-dimensional organization of telomeres in the nucleus of mammalian cells. *BMC Biol.* (2004). 2: 12-20.
53. Caporali, A.; Wark, L.; Vermolen, B. et al. Telomeric aggregates and end-to-end chromosomal fusions require myc box II. *Oncogene.* 2007. 26: 1398-1406.
54. Schaefer, L.; Schuster, D. & Herz, H. *J. Microsc.* 2001. 204(2): 99-107.
55. Sakharkar, M.K.; Perumal, B.S.; Sakharkar, K.R. et al. An analysis on gene architecture in human and mouse genomes. *In Silico Biol.* (2005). 5(4): 347-65.
56. Bianchi, N.O. Y chromosome structural and functional changes in human malignant diseases. *Mutat Res.* (2009). 682(1): 21-7.
57. Pageau, G.J.; Hall, L.L.; Ganesan, S. The disappearing Barr body in breast and ovarian cancers. *Nat Rev Cancer.* (2007). 7(8): 628-33.
58. Upender, M.B.; Habermann, J.K.; McShane L.M. et al. Chromosome transfer induced aneuploidy results in complex dysregulation of the cellular transcriptome in immortalized and cancer cells. *Cancer Res.* (2004). 64(19): 6941-9.

Figures

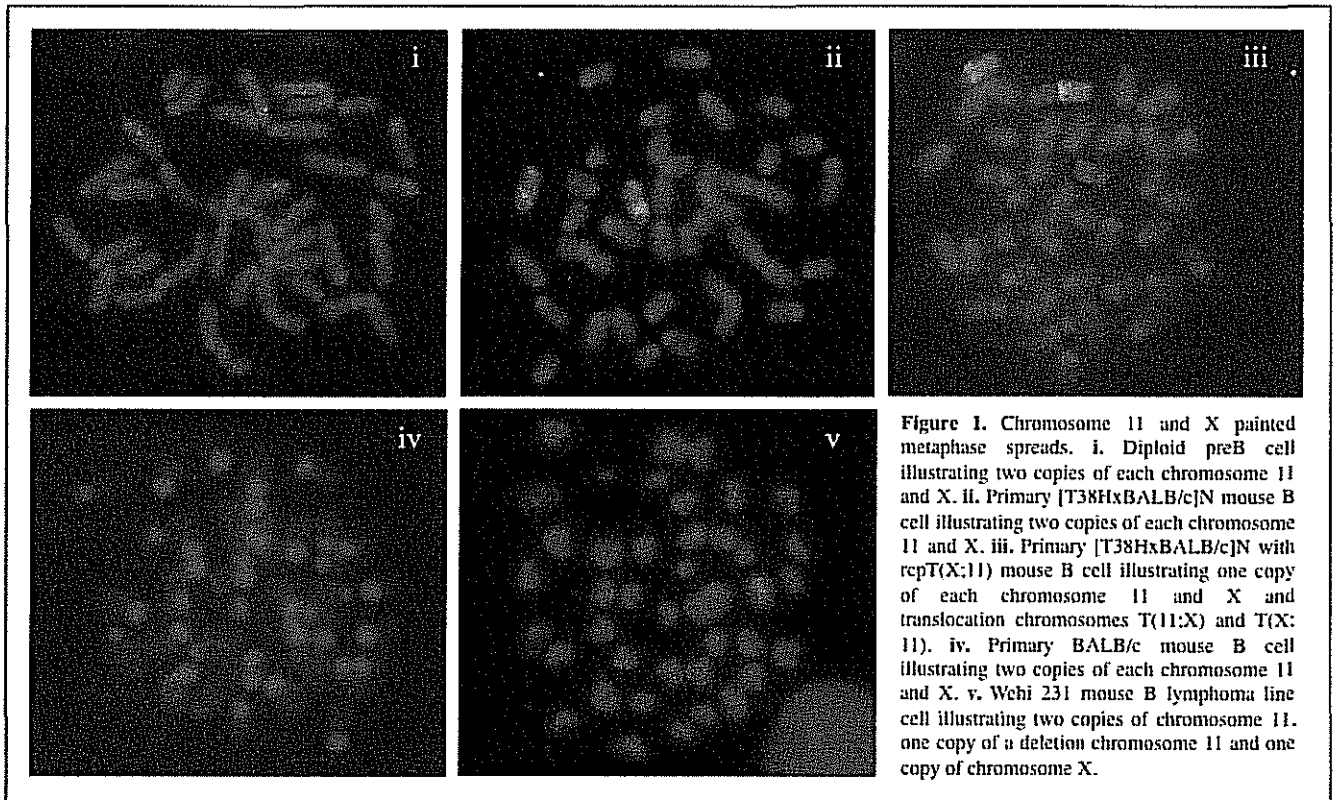


Figure I. Chromosome 11 and X painted metaphase spreads. i. Diploid preB cell illustrating two copies of each chromosome 11 and X. ii. Primary [T38HxBALB/c]N mouse B cell illustrating two copies of each chromosome 11 and X. iii. Primary [T38HxBALB/c]N with repT(X:11) mouse B cell illustrating one copy of each chromosome 11 and X and translocation chromosomes T(11:X) and T(X:11). iv. Primary BALB/c mouse B cell illustrating two copies of each chromosome 11 and X. v. Wehi 231 mouse B lymphoma line cell illustrating two copies of chromosome 11, one copy of a deletion chromosome 11 and one copy of chromosome X.

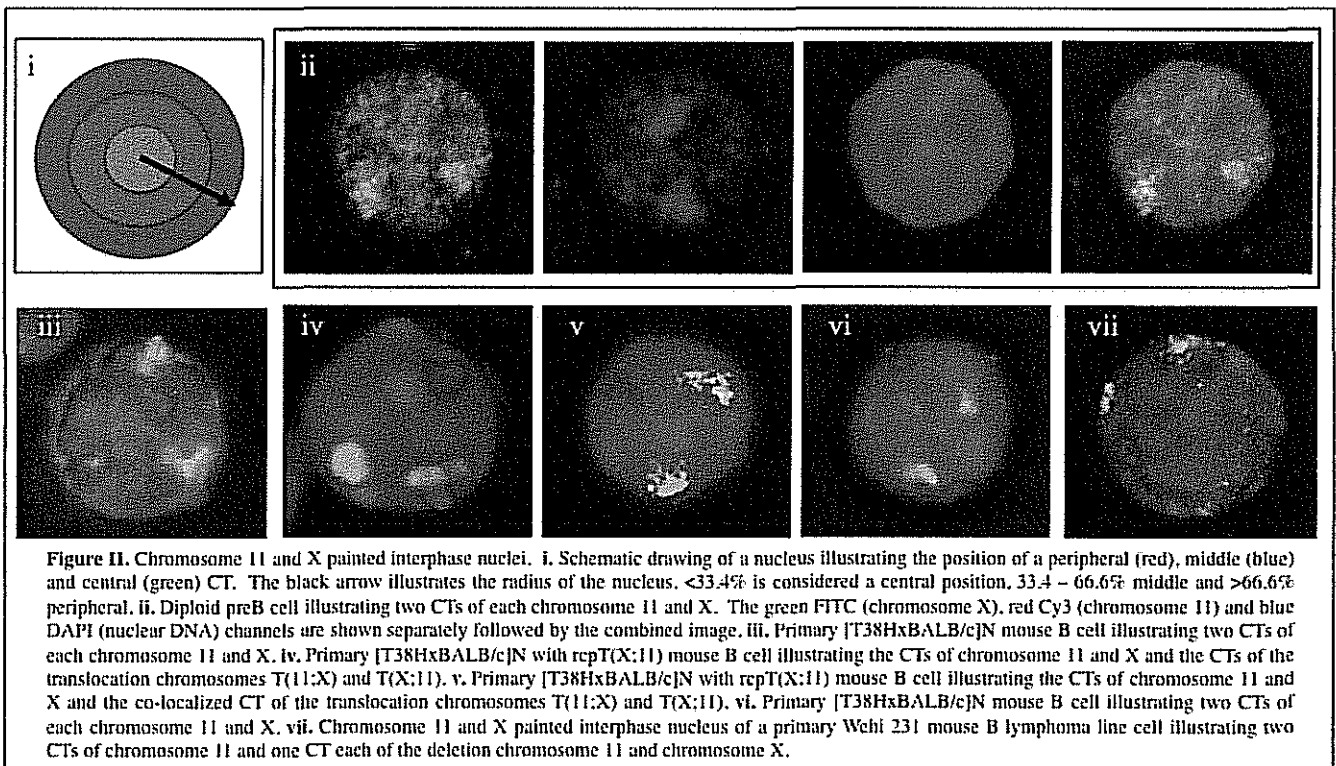


Figure II. Chromosome 11 and X painted interphase nuclei. i. Schematic drawing of a nucleus illustrating the position of a peripheral (red), middle (blue) and central (green) CT. The black arrow illustrates the radius of the nucleus. <33.4% is considered a central position, 33.4 - 66.6% middle and >66.6% peripheral. ii. Diploid preB cell illustrating two CTs of each chromosome 11 and X. The green FITC (chromosome X), red Cy3 (chromosome 11) and blue DAPI (nuclear DNA) channels are shown separately followed by the combined image. iii. Primary [T38HxBALB/c]N mouse B cell illustrating two CTs of each chromosome 11 and X. iv. Primary [T38HxBALB/c]N with repT(X:11) mouse B cell illustrating the CTs of chromosome 11 and X and the CTs of the translocation chromosomes T(11:X) and T(X:11). v. Primary [T38HxBALB/c]N with repT(X:11) mouse B cell illustrating the CTs of chromosome 11 and X and the co-localized CT of the translocation chromosomes T(11:X) and T(X:11). vi. Primary [T38HxBALB/c]N mouse B cell illustrating two CTs of each chromosome 11 and X. vii. Chromosome 11 and X painted interphase nucleus of a primary Wehi 231 mouse B lymphoma line cell illustrating two CTs of chromosome 11 and one CT each of the deletion chromosome 11 and chromosome X.

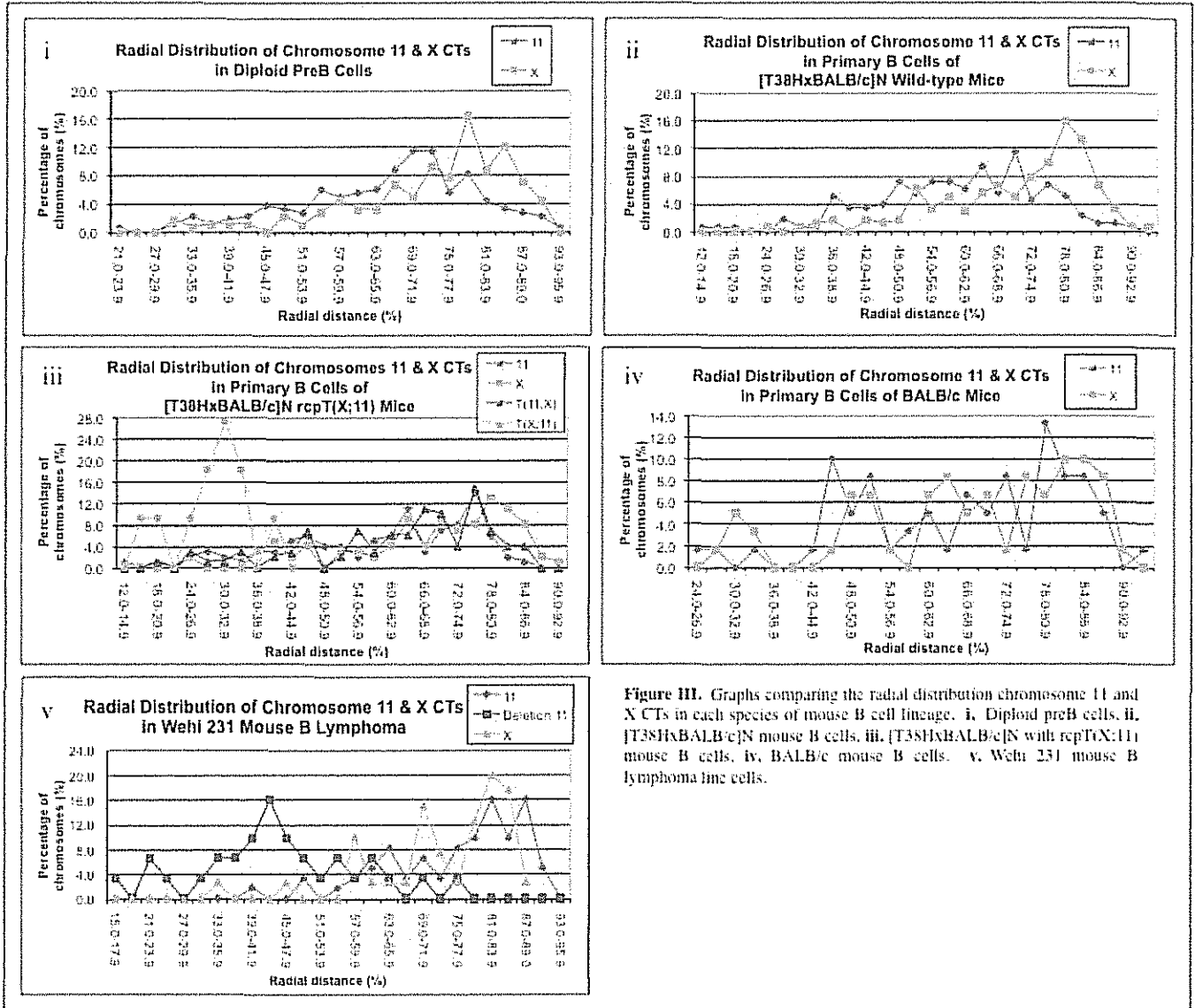
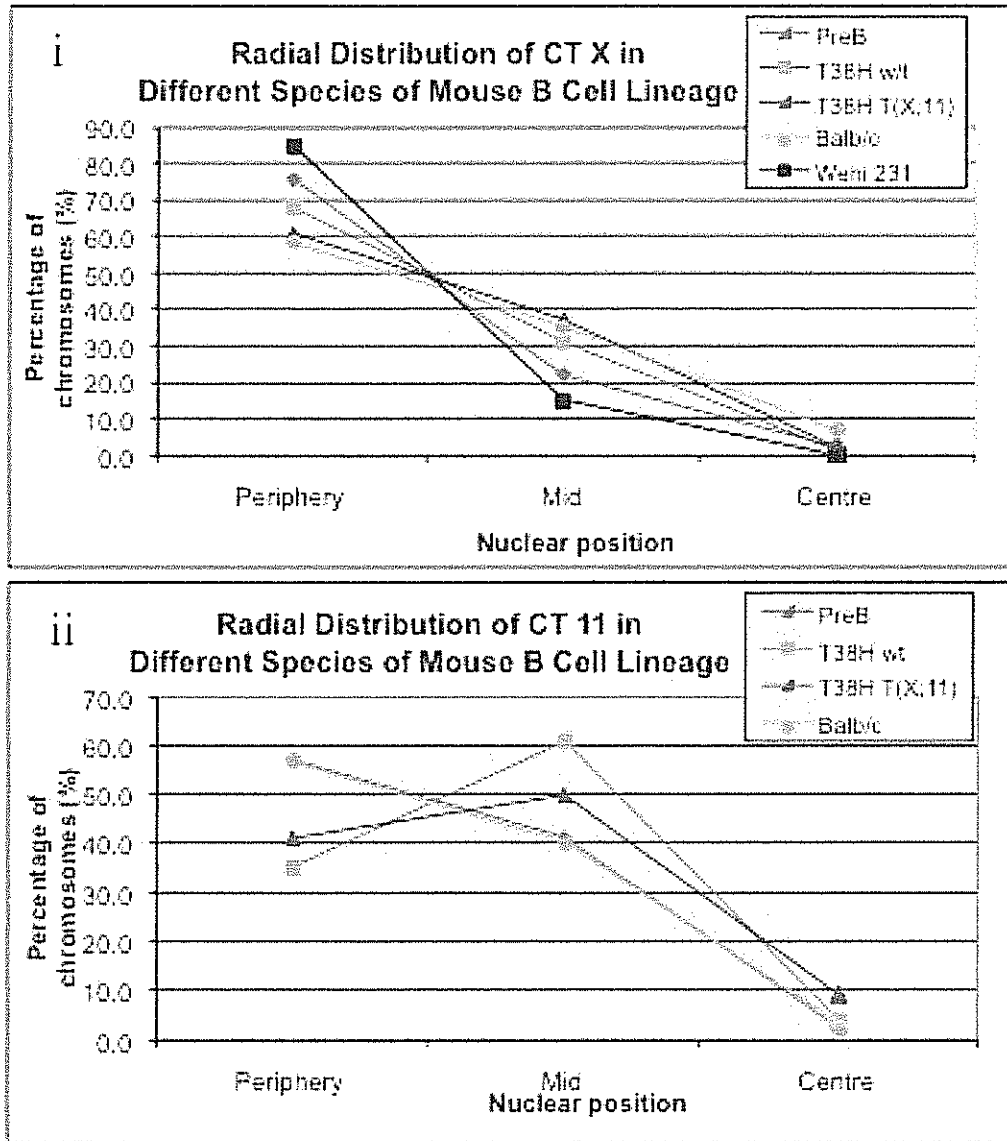
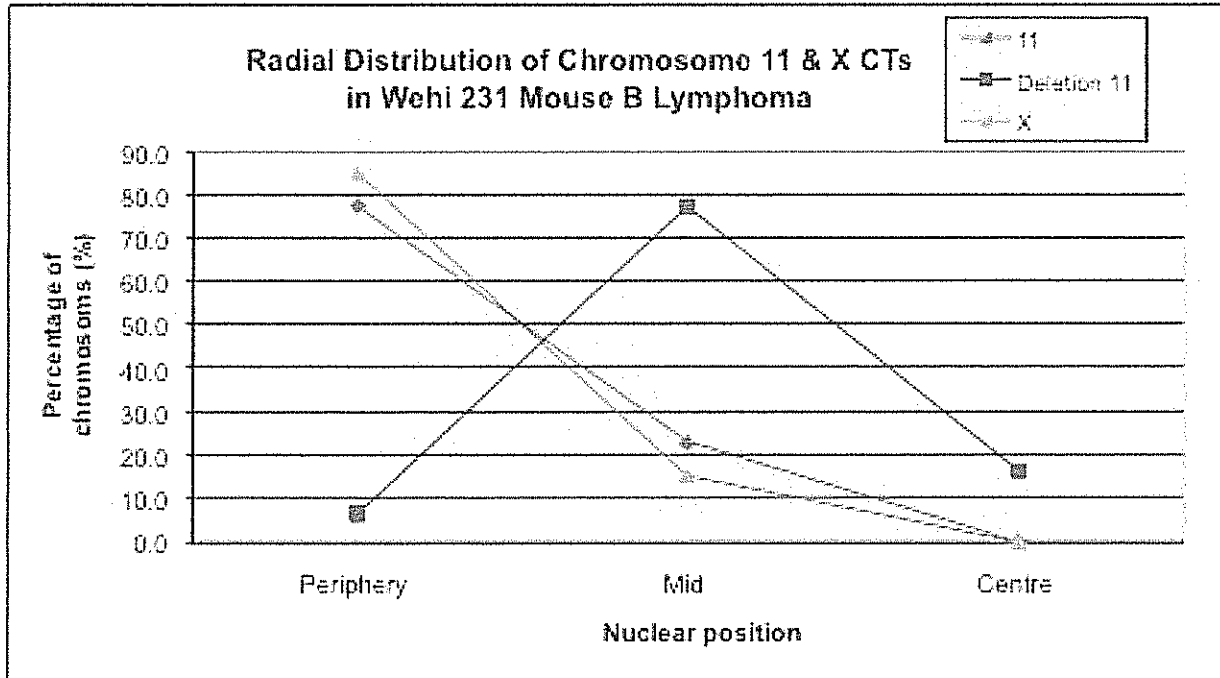


Figure III. Graphs comparing the radial distribution chromosome 11 and X CTs in each species of mouse B cell lineage. i, Diploid preB cells. ii, [T38HxBALB/c]N mouse B cells. iii, [T38HxBALB/c]N with rcpT(X;11) mouse B cells. iv, BALB/c mouse B cells. v, Wehi 231 mouse B lymphoma line cells.



**Figure IV.** Graphs comparing the radial distribution of CTs across all species of mouse B cell lineage. i. CT X. ii. CT 11.



**Figure V.** Graph comparing the radial distribution of CTs in Wehi 231 mouse B lymphoma line cells.